NASA TN D-360

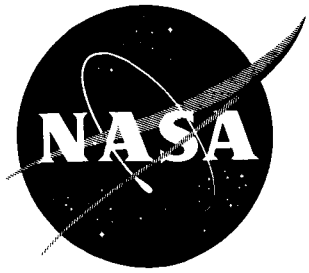

TECHNICAL NOTE
D-360

BENDING AND COMPRESSION TESTS OF PRESSURIZED RING-STIFFENED CYLINDERS

By Marvin B. Dow and James P. Peterson

Langley Research Center
Langley Field, Va.

NATIONAL AERONAUTICS AND SPACE ADMINISTRATION

WASHINGTON April 1960

NATIONAL AERONAUTICS AND SPACE ADMINISTRATION

TECHNICAL NOTE D-360

BENDING AND COMPRESSION TESTS OF PRESSURIZED RING-STIFFENED CYLINDERS

By Marvin B. Dow and James P. Peterson

SUMMARY

The results of tests on pressurized ring-stiffened cylinders subjected to compression and bending are presented and discussed. The results obtained at high values of internal pressure differ from those obtained by previous investigators in that the theoretical small-deflection compressive buckling coefficient of 0.6 was nearly achieved in each test. Small amounts of internal pressure had a greater stabilizing effect in the bending tests than in the compression tests.

INTRODUCTION

The pressurized ring-stiffened thin-walled cylinder can be used effectively as a fuselage for aircraft or missiles if the expected airloads and maneuver loads are small. If the loads are sufficiently small, a membrane can be used which derives its stabilization entirely from internal pressure. For larger loads the cylinder itself provides some stabilization. It is on this latter range that considerable interest has recently been focused, with the result that several test series on pressurized cylinders have been conducted. (See refs. 1 to 6.)

Practically all previous tests have been made on single-bay specimens clamped at each end to heavy fixtures. In some cases the specimens were small. In other cases the specimens were constructed from materials which develop some plasticity at very low stress levels. Experience in testing unpressurized cylinders has indicated that the results of tests on such cylinders may differ substantially from those obtained on larger ring-stiffened cylinders. (See ref. 7.)

Some of the results obtained to date on pressurized cylinders seem inconsistent with current explanations of cylinder behavior in that even large amounts of internal pressure did not stabilize the test cylinders to the extent that the theoretical small-deflection buckling stress was nearly achieved. The discrepancy between perfect-cylinder theory and experiment is usually associated with geometric imperfections

and associated stress concentrations. Large amounts of internal pressure should pull out imperfections that might have existed prior to pressurization and provide cylinders which are substantially in agreement with theory. Pressurization also induces axisymmetric radial deformations of the cylinder wall near the ends of the cylinder which may be looked upon as a type of imperfection. However, except for a bulging of the cylinder wall near the ends of the cylinder, these deformations are extremely small until the applied axial stress approaches the theoretical small-deflection buckling value.

In order to provide test data on cylinders lacking some of the objections discussed, tests were made on 30-inch-diameter ring-stiffened cylinders constructed of 7075-T6 aluminum alloy. The results of this investigation which include both bending and compression tests are reported herein.

L 8 8 1

SYMBOLS

E	Young's modulus, ksi
l	ring spacing, in.
p	internal pressure, ksi
$\frac{p}{E}\left(\frac{R}{t}\right)^2$	pressure parameter
R	radius of cylinder, in.
t	thickness of cylinder wall, in.
Z	curvature parameter, $\frac{l^2}{Rt}\sqrt{1 - \mu^2}$
σ	compressive stress in cylinder wall, ksi
$\frac{\sigma}{E}\frac{R}{t}$	stress coefficient
μ	Poisson's ratio

TEST SPECIMENS AND TEST PROCEDURES

Test Specimens

The test specimens consisted of twenty 30-inch-diameter ring-stiffened cylinders in which only the wall thickness and number of test bays per cylinder were varied from cylinder to cylinder. The cylinders were similar to those used in reference 7. Their dimensions are given in tables I and II. The rings of the test cylinders were of Z-section and were made by spinning. Dimensions of the rings and the means of attaching the rings to the cylinder wall are given in figure 1.

The bending cylinders with nominal wall thicknesses of 0.032 and 0.051 inch were constructed with the with-grain direction of the wall material in the circumferential direction and with a single longitudinal wall splice on the tension side of the cylinder. The remaining cylinders were constructed with three equally spaced wall splices and with the with-grain direction of the wall material in the axial direction. For the bending tests of cylinders with three wall splices, the cylinders were oriented so that the maximum compressive stress occurred between skin splices; and, no difficulty was experienced with the skin splices. However, in the compression tests, buckling sometimes seemed to emanate from the vicinity of a skin splice which consisted of a lap joint held together by a double row of rivets and Araldite cement. One of the two sections of skin comprising the joint was joggled in the early tests as is often done to provide a neater seam. These seams were later reinforced for the compression-test cylinders with the use of several layers of fiber-glass fabric bonded to the cylinder a layer at a time in an attempt to prevent the occurrence of buckling adjacent to seams. In addition, the longitudinal seams of the remaining cylinders were constructed without joggling one of the skins. A few of the cylinders constructed after the process of joggling one of the skins had been discontinued were also reinforced with fiber-glass fabric. This was done only if buckling seemed to occur near a longitudinal seam.

The cylinders were constructed of 7075-T6 aluminum alloy. Typical material properties were used in reducing the data. Young's modulus E was taken as 10,500 ksi and Poisson's ratio μ was assumed to be 0.32.

Test Procedures

The test setup for the bending tests is shown in the photograph of figure 2. The setup for the compression tests was similar except for the method of load application. The method of applying load to the compression cylinders is shown in figure 3. In either setup the

cylinders were pressurized with an oil having a specific gravity of 0.91 and with the use of a hydraulic pumping unit. Oil pressure was measured with a sensitive Bourdon tube pressure indicator. Corrections to the indicated pressure were made to account for the difference in elevation between the test section of the test cylinders and the pressure indicator. The pressure was corrected to the top of the cylinder for the bending tests and to the center of the uppermost full-length bay of the cylinder for the compression tests.

Prior to testing, several resistance-type wire strain gages were mounted on the cylinder at strategic locations on either side of the skin of the cylinders. Strains from the gages were autographically recorded during the test with the use of a 24-channel strain recorder. The strains were used to help detect cylinder buckling and to check on the uniformity of stress distribution in the cylinders; for compression cylinders with fiber-glass reinforcements along longitudinal seams, the buckling stress was deduced from the strain-gage readings because of the inherent uncertainties associated with determining the buckling stress from the applied load. The buckling stress was obtained by averaging the results of back-to-back gages at three equidistant locations around the cylinder. Strain-gage rosettes were used in place of linear strain gages in at least one of the three locations so that the effect of Poisson's expansion could be taken into account.

The procedure in each test was to pressurize the cylinder until the desired pressure was reached. The pressure was then held constant, and the applied load, either bending or compression, was increased until local buckles snapped into the cylinder wall. The load was then released and the procedure repeated. If the same buckling load was obtained in the second test, another pressure was selected and the process was repeated with the new pressure. The procedure was continued until all the data desired were obtained or until damage to the cylinder resulted so that loads could not be repeated. The latter was likely to occur with cylinders having small values of R/t that were tested at low values of internal pressure. It should be noted, however, that the behavior of oil-pressurized cylinders during buckling is rather favorable in protecting the cylinders from damage due to the large postbuckling deformations that ordinarily would occur. The internal volume of the test cylinders was apparently less in the buckled state than in the unbuckled state, so that buckling, which occurred suddenly with a slight snap-through effect, was accompanied by a moderate increase in internal pressure as well as by a small decrease in applied load and a small increase in shortening. The increase in internal pressure had the effect of stabilizing the cylinders (that is, increasing the buckling strength of the cylinders) as well as of relieving the cylinders of some axial stress (that is, more of the applied load was carried by pressure acting against the ends of the cylinder).

Load in the compression tests was applied through a ball-and-socket arrangement on top of the cylinder (fig. 3) in an attempt to obtain a uniform distribution of stress around the circumference of the cylinder. Readings from the strain gages indicated that the stress distribution prior to buckling was reasonably uniform. The indicated strains in the cylinders at three locations around the circumference of a test bay usually differed by less than 5 percent and always differed by less than 10 percent. In computing the compressive stress in the cylinders the following factors were taken into account: (1) the weight of the ball-and-socket arrangement and other fixtures on the upper end of the cylinder, (2) the tension load in the cylinder resulting from oil pressure on the upper-end fixture, and (3) the contribution of the three skin splices to the resisting area of the cylinder wall.

Load in the bending tests was applied through a loading frame which converted jack load to bending moment. (See fig. 2.) The presence of other loads in the test cylinders was minimized as far as practicable by employing rollers between moving surfaces and by counterbalancing fixtures near their center of gravity. Rollers were used between the loading frame and the floor supports as well as between the loading frame and the testing machine to allow the cylinders to shorten during loading and to restrict the loads at these locations to normal loads. The rollers were case hardened as were the surfaces against which they reacted. Stray loads not eliminated by counterbalancing and by the use of rollers were considered in reducing the data, including a 4-percent correction for friction which has been determined to be a representative value for the loading frame. Half of the weight of the oil was counterbalanced at the tip of the cylinder. The other half was supported by the massive backstop to which the cylinders were attached. This resulted in a bending moment in the cylinders which had a maximum value at the center of the cylinder. In addition to this moment, the pressurized oil loaded the cylinder in tension as it did in the compression case and applied a small bending moment to the cylinder because of the change in internal pressure with changes in elevation. These moments and loads were considered in determining the compressive extreme fiber stress in the test cylinders.

TEST RESULTS AND DISCUSSION

Results of the tests are given in tables I and II and in figures 4 and 5 in terms of the buckling stress coefficient $\frac{\sigma}{E}\frac{R}{t}$ and the pressure parameter $\frac{p}{E}\left(\frac{R}{t}\right)^2$. The buckling coefficient is the usual one for moderately long isotropic cylinders, and the pressure parameter has the

significance of being the theoretical unrestrained growth of the cylinder radius in sheet thicknesses resulting from the pressure p. Hence, with a pressure parameter of unity the radius of the cylinder should be increased by a sheet thickness because of hoop tension. Another useful significance can be associated with the pressure parameter. The ratio of hoop tensile stress $p\frac{R}{t}$ to the small-deflection buckling stress $\frac{E}{\sqrt{3(1 - \mu^2)}} \frac{t}{R}$ is $\sqrt{3(1 - \mu^2)}$ times the pressure parameter. Hence, the pressure parameter is approximately 0.61 times the ratio of the hoop tensile stress to the classical buckling stress of the cylinder.

The compression tests will be discussed first because they are helpful in interpreting the results of the bending tests.

Compression Tests

The theoretical small-deflection buckling stress was nearly achieved in the compression tests (fig. 4) when sufficiently large values of internal pressure were used. In the worst case a value of about 0.55 was actually obtained instead of the theoretical value of 0.61. Discrepancies of this magnitude would seem to be a likelihood for such tests because, as mentioned earlier, pressure-induced radial deformations commence growing at axial stresses approaching the theoretical buckling stress. These deformations may act as imperfections and induce buckling at loads somewhat less than the theoretical value.

Experimental errors are expected to be somewhat greater for tests of pressurized cylinders than for tests of nonpressurized cylinders. Errors in measuring two quantities (load and pressure) are involved in the pressurized cylinder tests instead of a single quantity (load), and the measured buckling coefficient is a function of the difference of parameters containing these quantities. This could result in particularly poor accuracy for cylinders having ratios of radius to thickness larger than those reported herein that are tested at high values of internal pressure where most of the stabilization against buckling is derived from internal pressure. In the present tests at least half of the applied load was carried in the walls of the test cylinder.

Scatter in the results presented is not large except for that shown in figure 4(b), where the results for cylinder 2A are particularly low for small values of internal pressure. The behavior of this cylinder as indicated by strain-gage output was different from the rest of the cylinders, even though the cylinder was not visibly of inferior quality. For the other cylinders the indicated load-strain relationship was

nearly linear until buckling which occurred with a slight snap-through action and which was accompanied by abrupt changes in indicated strain. For cylinder 2A the indication was that a buckle commenced developing in the vicinity of one of the strain gages early in the test; at a load somewhat less than the indicated buckling load, the buckle had developed to the extent that strain reversal (ref. 8) had occurred. Buckling when it finally occurred was accompanied by a snap-through action which was smaller than usual.

Other investigators have not obtained the theoretical small-deflection buckling coefficient at large values of internal pressure. (See refs. 2, 3, 5, and 6.) The reason for this discrepancy between previous tests and the present tests is not known. However, some differences in test specimens and test techniques are evident. The present specimens differ from those used in previous investigations in that the present specimens consisted of ring-stiffened cylinders comprising a test section of two or more bays and two buffer bays, one on either end of the test section. The buffer bays were short enough to be free of buckling. The specimens of other investigations were generally single-bay specimens clamped at each end to heavy fixtures. The test results of the two types of specimens are known to differ substantially for the zero-pressure case (ref. 7), but why they should differ for the case of large internal pressures has not been explained. The values of R/t covered by previous tests were somewhat larger than those covered by the present tests. Values of R/t comparable to those considered herein are reported in references 1 and 2, but data are not given for large values of internal pressure where the theoretical buckling coefficient might have been attained.

An important difference may be that of the wall material of the test cylinders. There is some evidence of plasticity in some of the previous tests which were made on cylinders of low-strength aluminum alloys or of half-hard stainless steel, which has a rather rounded stress-strain curve, whereas there is no evidence of plasticity in the present tests. In the investigations of references 2, 3, and 6, axisymmetric radial deformations were clearly visible over large portions of the test cylinders at high internal pressures and at loads considerably less than the theoretical buckling load. Elastic theory (ref. 9) indicates that such deformations should remain small until the theoretical buckling load is approached. However, such deformations would be evident earlier if the proportional limit of the material under the biaxial stress conditions present were exceeded and, if present, the deformations might induce local buckling at a lower stress level. The proportional limit of the wall material was likely exceeded for some of the tests of references 2 and 3, but perhaps not exceeded in the tests of reference 6. Also, the proportional limit was evidently exceeded in the tests of reference 5 where the buckling load is shown to decrease with an increase in internal pressure.

The test procedure of previous investigations was sometimes different from that employed in the present investigation. A notable example is evident in table 1 of reference 3 where data are given for a cylinder after the cylinder had been apparently damaged by a previous test. (See tests 3(6) and 3(8).) In the present tests, the cylinder was assumed to be damaged in a test if the buckling load could not be repeated in a rerun of the test, and no further data were taken. Finally, it might be noted that some of the test setups were considerably different from the present test setup. (Note, particularly, those of refs. 2 and 3.)

The changes in buckle pattern associated with changes in internal pressure observed in the present tests were similar to those reported by other investigators. That is, as the pressure was increased from zero to a large value the buckle configuration changed from the familiar nearly equal-sided diamond-shaped buckles having rather severe bending distortions around their perimeter to buckles more elongated circumferentially and having more moderate radii of curvature around the perimeter of the buckle. (These types of buckles are referred to herein as local buckles.) At the higher pressures where the theoretical buckling coefficient was nearly achieved, an axisymmetric mode consisting of a corrugatedlike surface with the corrugations running circumferentially was evident prior to buckling in the local mode. (This mode is referred to herein as the axisymmetric mode.) As additional shortening was applied to the cylinder in the axisymmetric mode, it was replaced by a local mode in which the longitudinal wavelength of buckles was nearly that of the axisymmetric mode which it replaced. The photographs of figure 6 display these buckling patterns for one test cylinder. Figure 7 shows the final buckling pattern in another test cylinder as it appeared after having been loaded considerably beyond buckling so as to accentuate the buckling pattern.

The behavior of the test cylinders was different at different values of internal pressure. At low values of internal pressure, buckling occurred rather abruptly with appreciable shortening of the cylinder; whereas, at higher values of internal pressure, buckling occurred more gradually and was accompanied by less shortening. At high values of internal pressure, axisymmetric deformations became visible near the rings at loads somewhat less than the buckling load. The cylinder in this state of deformation was in stable equilibrium and further increases in load resulted in an accentuation of the axisymmetric pattern as well as a spread of the visible pattern to areas farther from the rings. When the load approached the theoretical buckling load, the pattern was usually visible over the entire cylinder and at slightly higher loads was replaced by local buckles as just discussed. Cylinder behavior in the present tests differed from that of other investigations in that deformations in the axisymmetric mode were not in any case

clearly visible over a large portion of the cylinder until the theoretical small-deflection buckling load was approached.

Bending Tests

Results of the bending tests are given in figure 5. The buckling coefficients given are for the extreme compression fiber of the cylinder and were obtained using the original section modulus (I/c) of the cylinder. Two values of stress coefficient are given in some cases for high values of internal pressure. The upper value corresponds to local buckling of the cylinder, and the lower value corresponds to strain reversal (ref. 8) in the cylinder wall at the longitudinal center line of a test bay of the cylinder. The strain-reversal values are given because they are indicative of cylinder behavior at high pressures where radial deformations in the axisymmetric mode (a misnomer in the bending case) are significant.

The values of stress coefficient shown for strain reversal correspond closely to the theoretical buckling coefficient of the cylinder and represent the beginning of large deformations in the axisymmetric mode. At loads corresponding to strain reversal, radial deformations had grown to the extent that they were visible over practically the entire bay length of the cylinder in the region of maximum compressive stress. At corresponding loads for the compression tests discussed previously, the axisymmetric deformations grew rapidly with a corresponding growth in cylinder shortening for small increases in applied load until local buckling occurred. The same action is believed to have occurred here. That is, the axial stress in the cylinder wall at the extreme compression fiber probably did not change appreciably between the loads represented by strain reversal and local buckling. The large change in stress shown really represents a change in applied moment. The moment increased without increasing the stress in the extreme compression fiber because the distribution of stress in the cylinder changed with the side walls of the cylinder taking more of the load. The action is similar to that of a cylinder in which the compressive stresses exceed the proportional limit of the wall material; use of the stress coefficient in the present application is equivalent to the use of the familiar "rupture coefficient" in the plastic case. Strain-reversal points are not given for cylinders with small values of the curvature parameter Z because strain reversal at the center of a bay for such cylinders occurs early and does not represent the load at which axisymmetric deformations commence growing rapidly with small increases in applied load.

A comparison of the results shown in figures 4 and 5 indicates that small amounts of internal pressure are more effective in stabilizing the cylinder wall to withstand increases in compressive stresses in the bending case than in the compression case. For example, for a cylinder

in bending with 0.020-inch wall thickness, an internal pressure of approximately 6 psi was required to stabilize the cylinder so that the theoretical compressive buckling stress was nearly obtained. For the cylinder in compression, an internal pressure of approximately 15 psi was required.

CONCLUDING REMARKS

The results of bending and compression tests of pressurized ring-stiffened circular cylinders are presented. Unlike the results of previous investigations the theoretical buckling coefficient of 0.6 was nearly achieved in all tests at high values of internal pressure. More pressure was required in the compression tests than in the bending tests to achieve the coefficient of 0.6. The prebuckling deformations were large at high values of internal pressure and consisted of a corrugated-like surface with the corrugations running circumferentially.

Langley Research Center,
National Aeronautics and Space Administration,
Langley Field, Va., January 18, 1960.

REFERENCES

1. Lo, Hsu, Crate, Harold, and Schwartz, Edward B.: Buckling of Thin-Walled Cylinder Under Axial Compression and Internal Pressure. NACA Rep. 1027, 1951. (Supersedes NACA TN 2021.)

2. Fung, Y. C., and Sechler, E. E.: Buckling of Thin-Walled Circular Cylinders Under Axial Compression and Internal Pressure. Jour. Aero. Sci., vol. 24, no. 5, May 1957, pp. 351-356.

3. Harris, Leonard A., Suer, Herbert S., Skene, William T., and Benjamin, Roland J.: The Stability of Thin-Walled Unstiffened Circular Cylinders Under Axial Compression Including the Effects of Internal Pressure. Jour. Aero. Sci., vol. 24, no. 8, Aug. 1957, pp. 587-596.

4. Suer, Herbert S., Harris, Leonard A., Skene, William T., and Benjamin, Roland J.: The Bending Stability of Thin-Walled Unstiffened Circular Cylinders Including the Effects of Internal Pressure. Jour. Aero. Sci., vol. 25, no. 5, May 1958, pp. 281-287.

5. Connor, Jerome J., Jr.: Buckling Characteristics of Circumferentially Reinforced Thin Cylindrical Shells Subjected to Axial Compression and Internal Pressure. Rep. No. WAL TR 715/2, Watertown Arsenal Labs. (Watertown, Mass.), Aug. 1958.

6. Lofblad, Robert P., Jr.: Elastic Stability of Thin-Walled Cylinders and Cones With Internal Pressure Under Axial Compression. Tech. Rep. 25-29, (Contract No. Nonr-1841(22)), Aeroelastic and Structures Res. Lab., M.I.T., May 1959.

7. Peterson, James P.: Bending Tests of Ring-Stiffened Circular Cylinders. NACA TN 3735, 1956.

8. Hu, Pai C., Lundquist, Eugene E., and Batdorf, S. B.: Effect of Small Deviations From Flatness on Effective Width and Buckling of Plates in Compression. NACA TN 1124, 1946.

9. Timoshenko, S.: Theory of Elastic Stability. McGraw-Hill Book Co., Inc., 1936, pp. 423-425.

TABLE I.- DIMENSIONS AND TEST RESULTS OF COMPRESSION CYLINDERS

Cylinder	t, in.	$\frac{R}{t}$	$\frac{l}{R}$	Splice details	Test length, bays	$\frac{p}{E}\left(\frac{R}{t}\right)^2$	$\frac{\sigma}{E}\frac{R}{t}$
1A	0.0222	685	0.987	(a)	2	0.029	0.342
						.118	.383
						.207	.405
						.296	.428
						.386	.455
						.475	.483
						.564	.503
						.654	.527
						.743	.541
						.788	.554
						.832	.585
						.877	.585
						.922	.586
1B	.0221	688	.987	(a)	2	.029	.297
						.119	.356
						.209	.411
						.299	.451
						.390	.456
						.480	.490
						.570	.497
						.660	.508
						.705	.523
						.750	.528
						.796	.539
						.841	.538
						.886	.547
						.931	.552
						.976	.562
1C	.0212	717	.987	(a)	2	.031	.324
						.129	.421
						.227	.429
						.325	.460
						.423	.496
						.521	.517
						.619	.538
						.717	.570
						.761	.571
						.805	.577
						.849	.585
						.892	.583
						.936	.598
						.980	.604
2A	.0199	765	.493	(b)	2	.028	.164
						.140	.246
						.251	.304
						.362	.356
						.474	.395
						.585	.428
						.696	.457
						.807	.486
						.919	.517
						1.030	.538
						1.086	.548
						1.141	.554
						1.197	.555
						1.253	.558
						1.309	.559
2B	.0222	685	.493	(b)	2	.023	.246
						.111	.306
						.190	.353
						.279	.398
						.368	.424
						.457	.448
						.545	.457
						.634	.494
						.723	.517
						.812	.538
						.856	.550
						.901	.557
						.945	.571
						.989	.579
						1.034	.578
						1.078	.583

[a]Longitudinal wall splices consist of lap joints of joggled construction with fiber-glass reinforcement.

[b]Longitudinal wall splices consist of lap joints constructed without joggling wall.

TABLE I.- DIMENSIONS AND TEST RESULTS OF COMPRESSION CYLINDERS - Concluded

Cylinder	t, in.	$\frac{R}{t}$	$\frac{l}{R}$	Splice details	Test length, bays	$\frac{p}{E}\left(\frac{R}{t}\right)^2$	$\frac{\sigma}{E}\frac{R}{t}$
2C	0.0223	682	0.493	(b)	2	0.465	0.518
						.554	.530
3A	.0194	782	.246	(b)	2	.145	.433
						.263	.479
						.381	.512
						.499	.530
						.616	.549
						.734	.556
						.852	.560
						.911	.561
3B	.0194	782	.246	(b)	2	.027	.353
						.144	.449
						.262	.482
						.379	.518
						.496	.554
						.613	.578
						.730	.600
						.848	.614
						.906	.615
						.965	.613
						1.023	.615
						1.082	.617
						1.141	.616
3C	.0195	780	.246	(b)	2	.027	.321
						.143	.407
						.259	.459
						.376	.506
						.492	.532
						.608	.539
						.724	.558
						.840	.567
						.898	.565
						.957	.566
						1.015	.567
						1.073	.568
						1.131	.573
4A	.0327	465	.987	(c)	2	.669	.617
4B	.0328	463	.987	(c)	2	.421	.553

[b]Longitudinal wall splices consist of lap joints constructed without joggling wall.

[c]Longitudinal wall splices consist of lap joints with fiberglass reinforcement. Lap joints were constructed without joggling wall.

TABLE II.- DIMENSIONS AND TEST RESULTS OF BENDING CYLINDERS[a]

Cylinder	t, in.	$\frac{R}{t}$	$\frac{l}{R}$	Test length, bays	$\frac{p}{E}\left(\frac{R}{t}\right)^2$	$\frac{\sigma}{E}\frac{R}{t}$	
						Buckling	Strain reversal
5A	0.0191	795	0.987	3	0	0.359	
					.060	.450	
					.121	.502	
					.181	.543	
					.241	.575	0.538
					.302	.589	.539
					.362	.598	.541
					.423	.608	.553
					.483	.628	.546
					.543	.653	.560
					.603	.676	.578
					.664	.696	.577
5B	.0183	831	.987	3	0	.444	
					.081	.510	
					.147	.540	
					.213	.565	
					.279	.584	
					.345	.592	
					.411	.618	
5C	.0220	692	.987	3	0	.410	
					.046	.483	
					.092	.539	
					.137	.561	
					.182	.589	
					.228	.606	
					.274	.626	
					.319	.641	.610
					.364	.653	.617
					.410	.669	.605
					.456	.681	.602
					.501	.688	.621
					.547	.701	.627
					.593	.711	.637
					.638	.725	.635
					.684	.736	.636
					.730	.753	.628
6A	.0211	721	.493	6	0	.376	
					.050	.451	
					.099	.483	
					.149	.521	
					.198	.552	
					.248	.592	
					.297	.622	
					.347	.641	
					.396	.664	
					.495	.710	
7A	.0197	770	.246	12	0	.373	
					.057	.437	
					.113	.483	
					.169	.524	
					.226	.557	
					.282	.598	
					.339	.630	
					.395	.663	
					.452	.700	
					.508	.721	
					.565	.772	
					.678	.798	
					.790	.840	
					.903	.860	

[a]Longitudinal wall splices consist of lap joints of joggled construction without fiberglass reinforcement.

TABLE II.- DIMENSIONS AND TEST RESULTS OF BENDING CYLINDERS[a] - Concluded

Cylinder	t, in.	$\frac{R}{t}$	$\frac{l}{R}$	Test length, bays	$\frac{p}{E}\left(\frac{R}{t}\right)^2$	$\frac{\sigma}{E}\frac{R}{t}$	
						Buckling	Strain reversal
8A	0.0324	469	0.987	3	0	0.408	
					.042	.457	
					.084	.475	
					.126	.495	
					.168	.519	
					.210	.537	
					.252	.553	
					.293	.573	0.536
					335	.591	.551
					.377	.607	.587
					.419	.620	.600
					.461	.627	.597
					.503	.641	.609
					.545	.655	.605
8B	.0321	473	.987	3	0	.424	
					.043	.460	
					.085	.492	
					.128	.516	
					.171	.539	
					.213	.555	.527
					.256	.570	.533
					.298	.586	.549
					.341	.600	.545
					.384	.616	.543
					.426	.638	.540
					.469	.646	.547
					.511	.654	.543
					.554	.655	.560
					.597	.663	.561
					.640	.673	.544
8C	.0320	475	.987	3	.043	.500	
					.215	.547	
					.258	.575	
					.301	.587	
					.344	.591	
					.387	.596	
					.430	.636	
9A	.0523	291	.987	3	.121	.600	.581
					.242	-----	.586

[a]Longitudinal wall splices consist of lap joints of joggled construction without fiber-glass reinforcement.

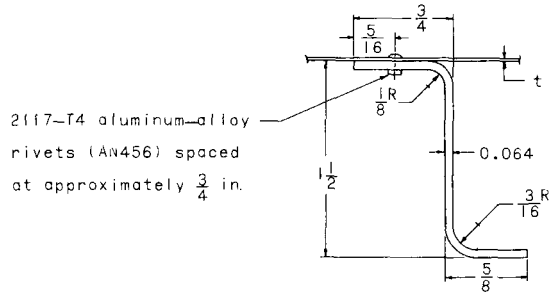

Diameter of ring attachment rivets	
Wall thickness, in.	Rivet diameter, in.
0.020	1/16
.032	3/32
.051	1/8

Figure 1.- Reinforcing rings of test cylinders.

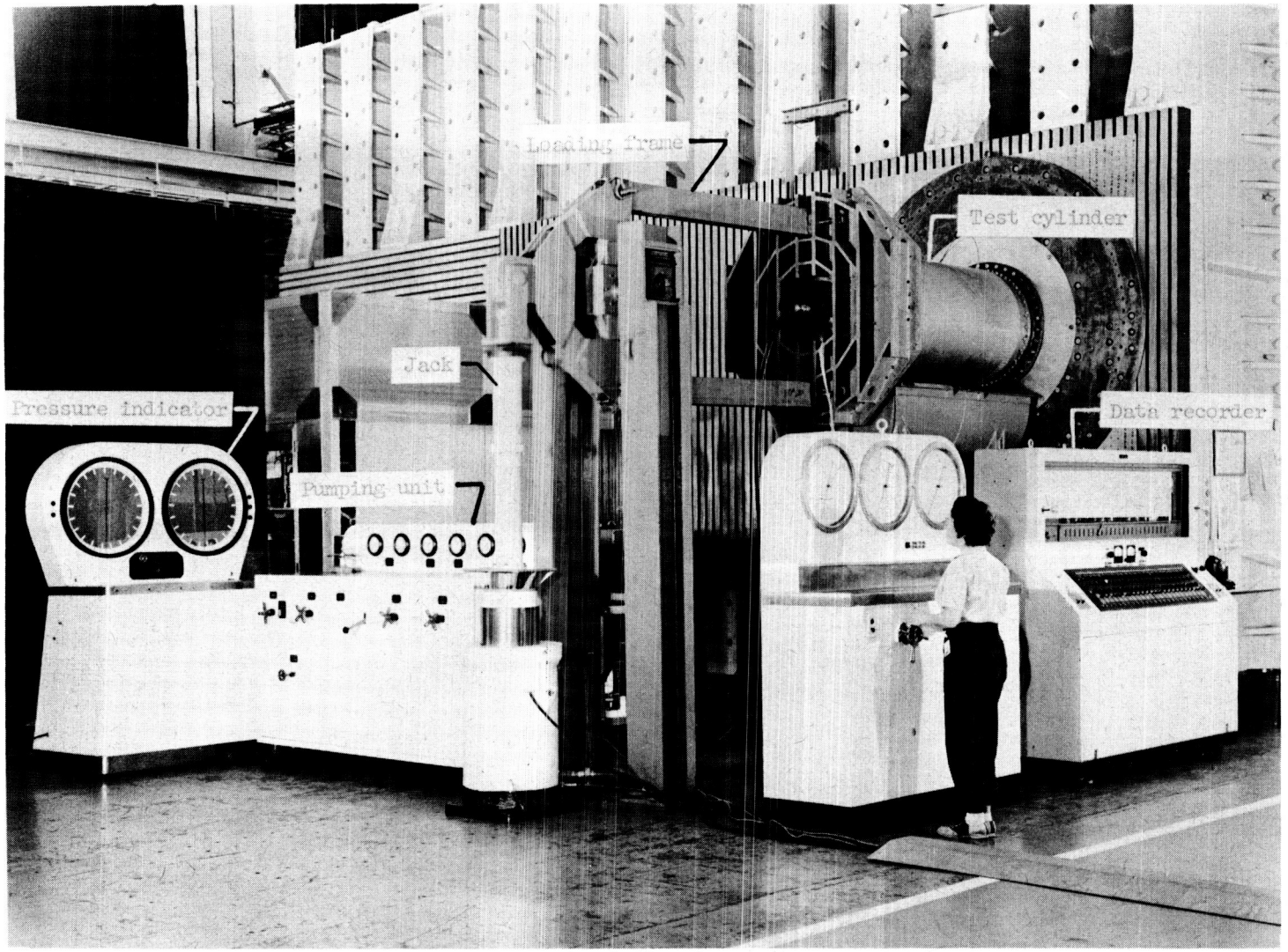

Figure 2.- Test setup for bending tests. L-59-6500.1

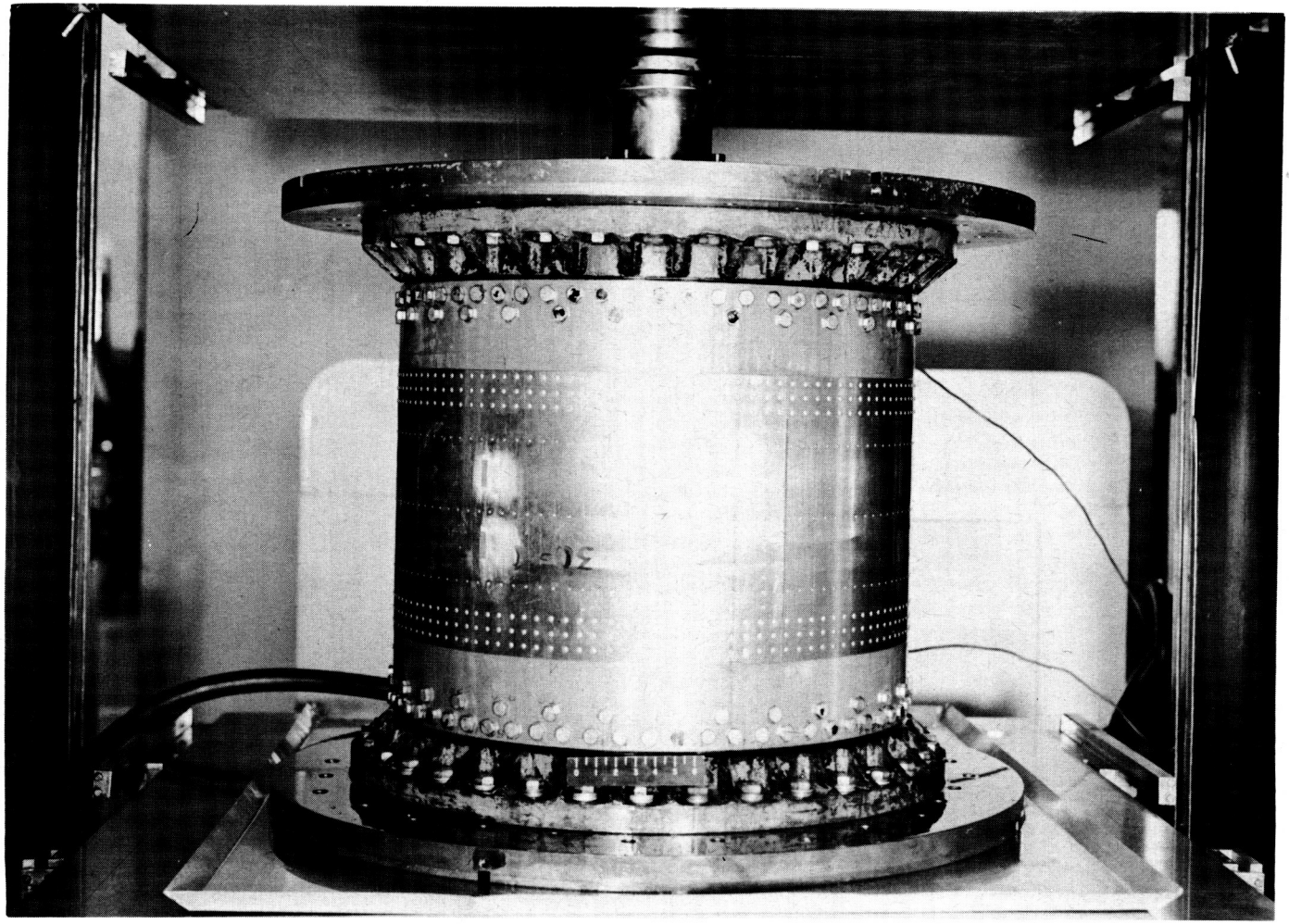

L-59-3722

Figure 3.- Method of applying load to the compression cylinders. Cylinder has been damaged by loading beyond buckling load.

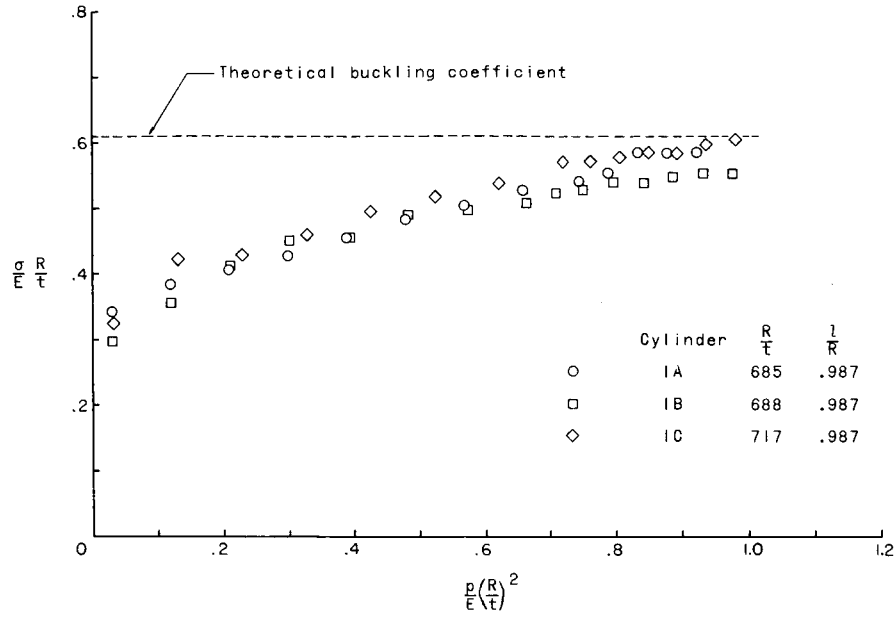

(a) Cylinder 1.

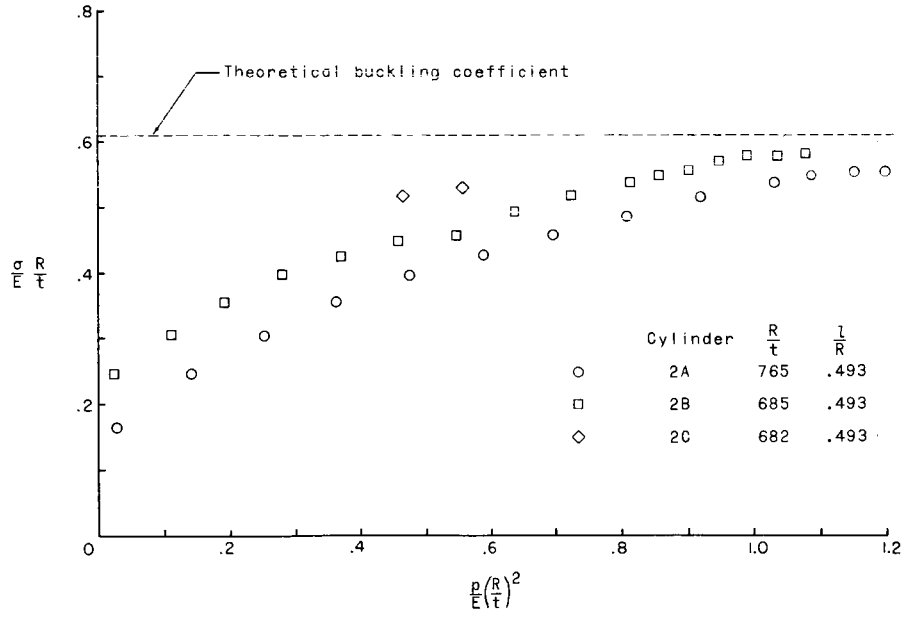

(b) Cylinder 2.

Figure 4.- Effect of internal pressure on the buckling coefficient for cylinders in compression.

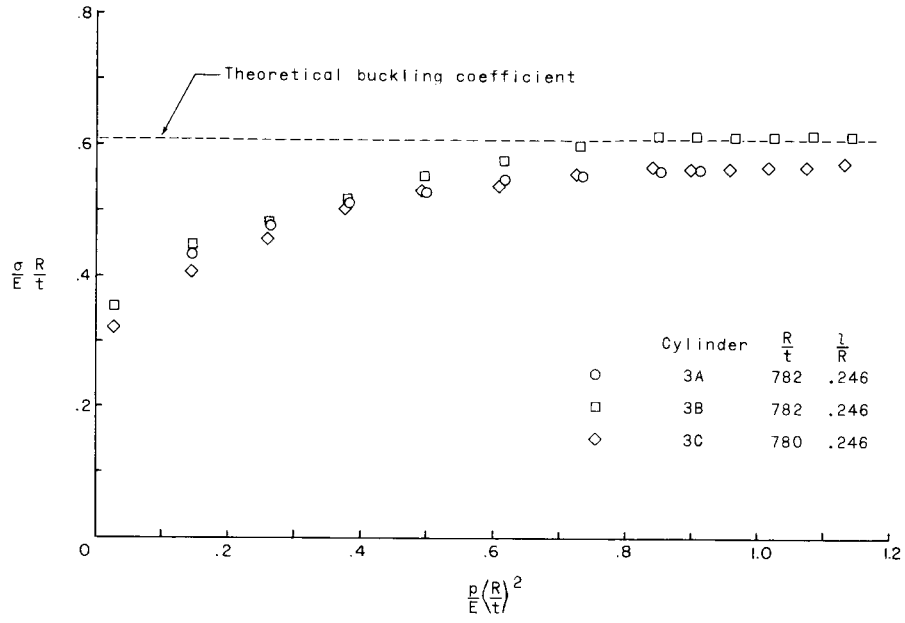

(c) Cylinder 3.

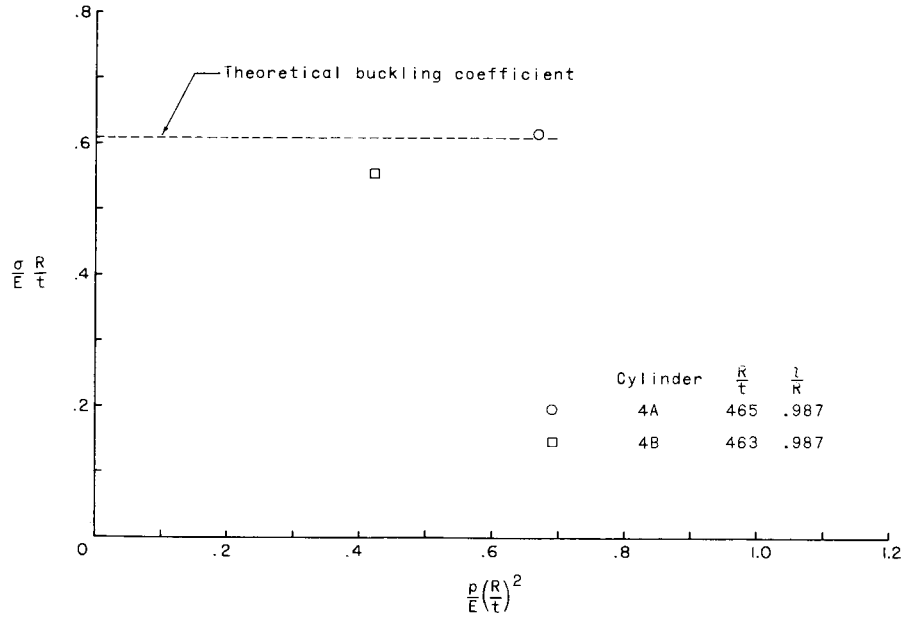

(d) Cylinder 4.

Figure 4.- Concluded.

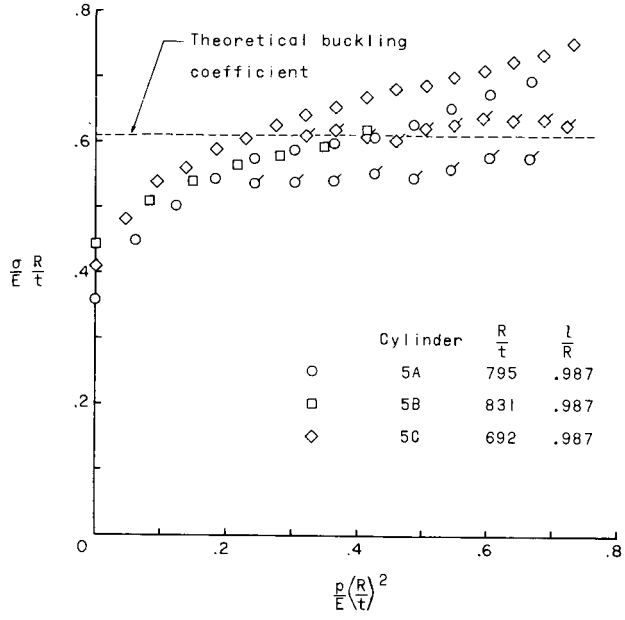

(a) Cylinder 5.

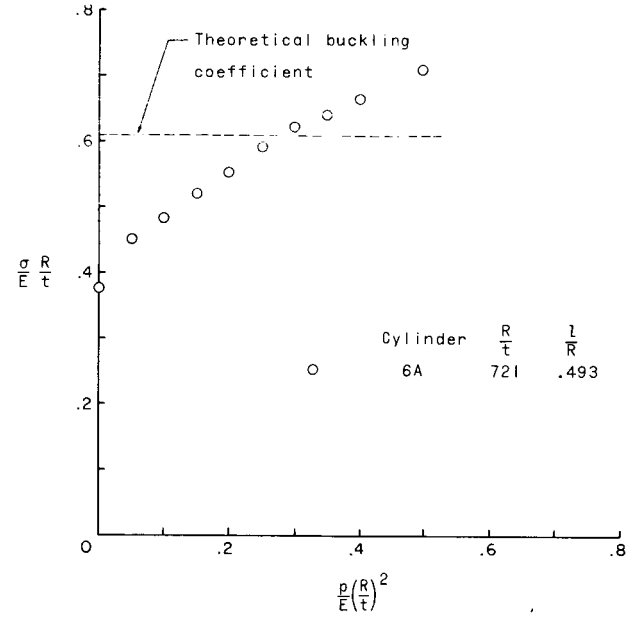

(b) Cylinder 6A.

Figure 5.- Effect of internal pressure on the buckling coefficient for cylinders in bending. Symbols with tails denote strain-reversal stresses.

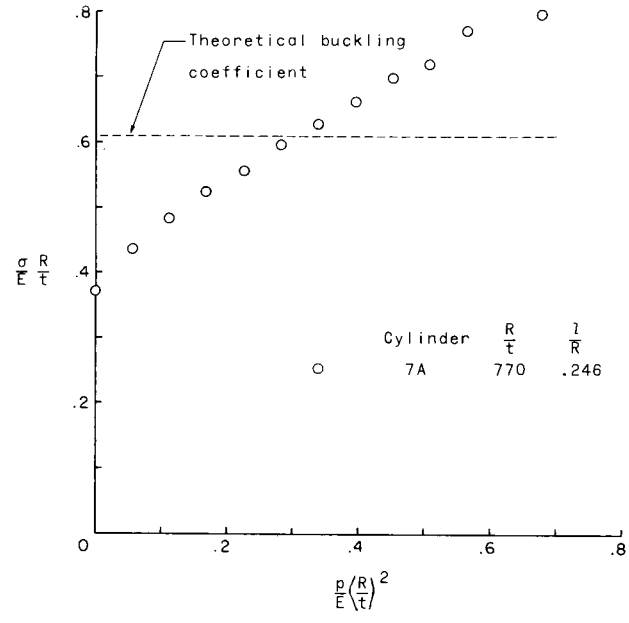

(c) Cylinder 7A.

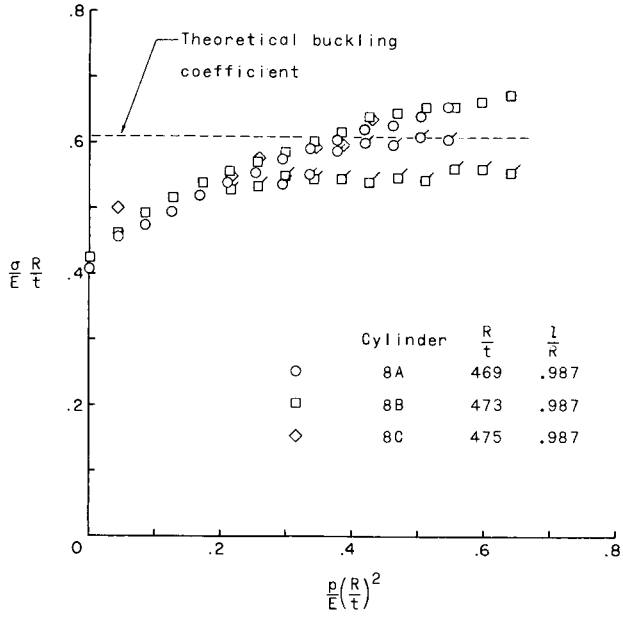

(d) Cylinder 8.

Figure 5.- Continued.

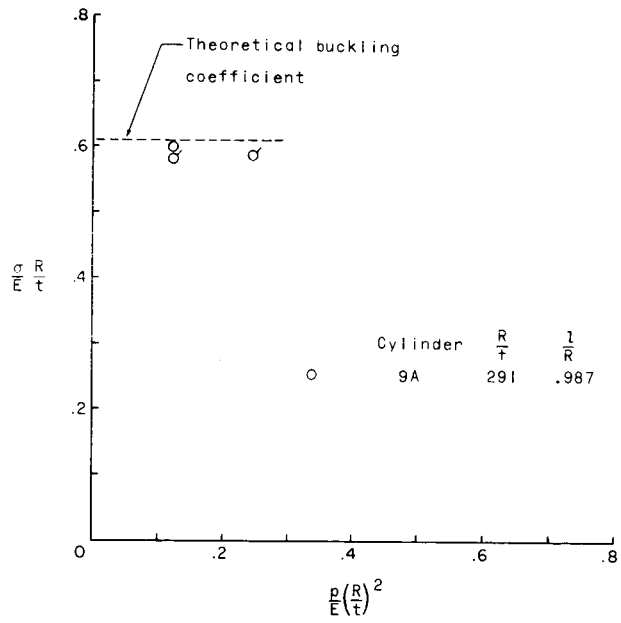

(e) Cylinder 9A.

Figure 5.- Concluded.

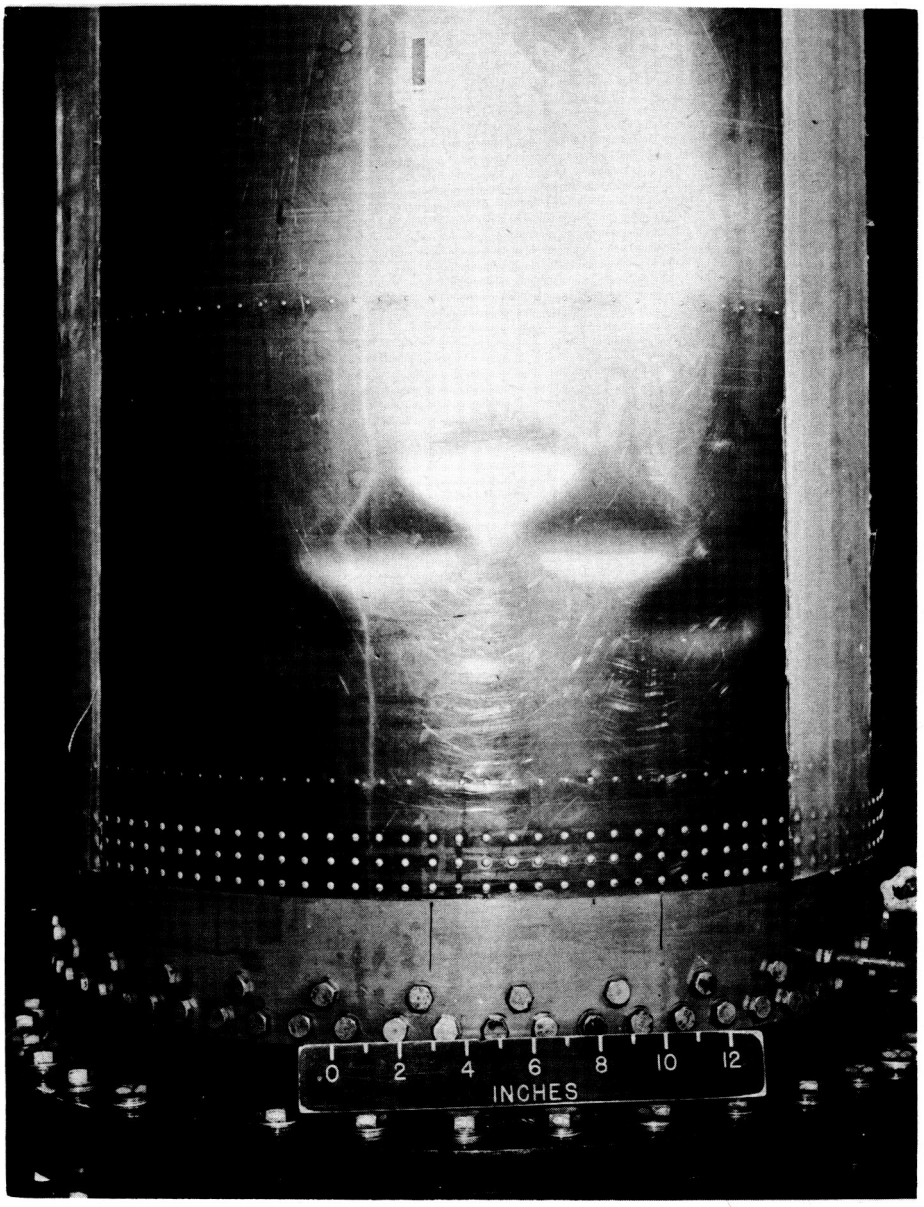

L-59-2984

(a) Local buckling at low value of internal pressure. $\frac{\sigma}{E}\frac{R}{t} = 0.356$; $\frac{p}{E}\left(\frac{R}{t}\right)^2 = 0.119$.

Figure 6.- Buckling of pressurized cylinder in compression. $\frac{R}{t} = 688$; $\frac{l}{R} = 0.987$. (Note fiber-glass reinforcement of longitudinal seams.)

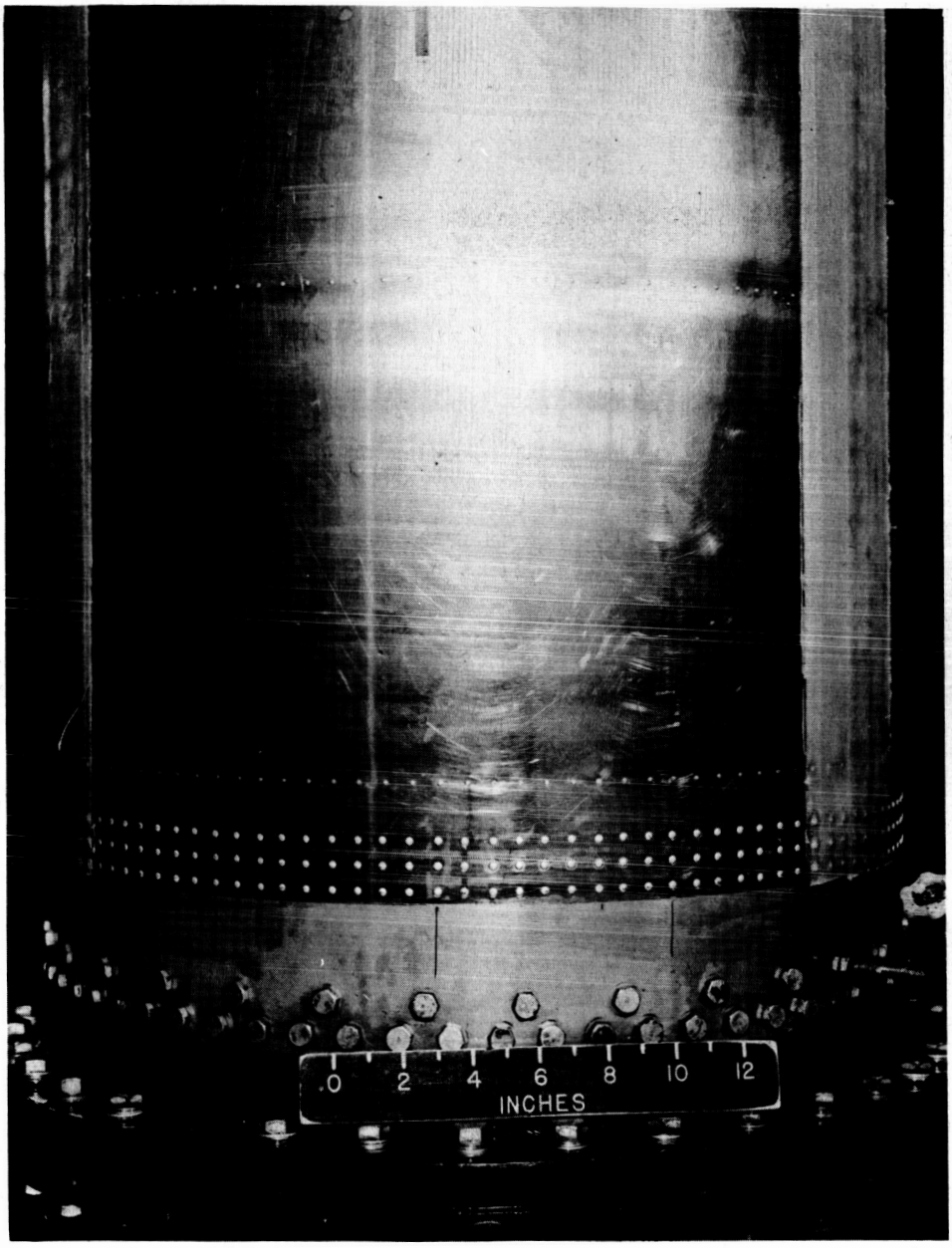

L-59-2982

(b) Axisymmetric deformations of cylinder wall at a large value of internal pressure and at a large value of applied load.

$\frac{\sigma}{E}\frac{R}{t} = 0.540$; $\frac{p}{E}\left(\frac{R}{t}\right)^2 = 0.931$.

Figure 6.- Continued.

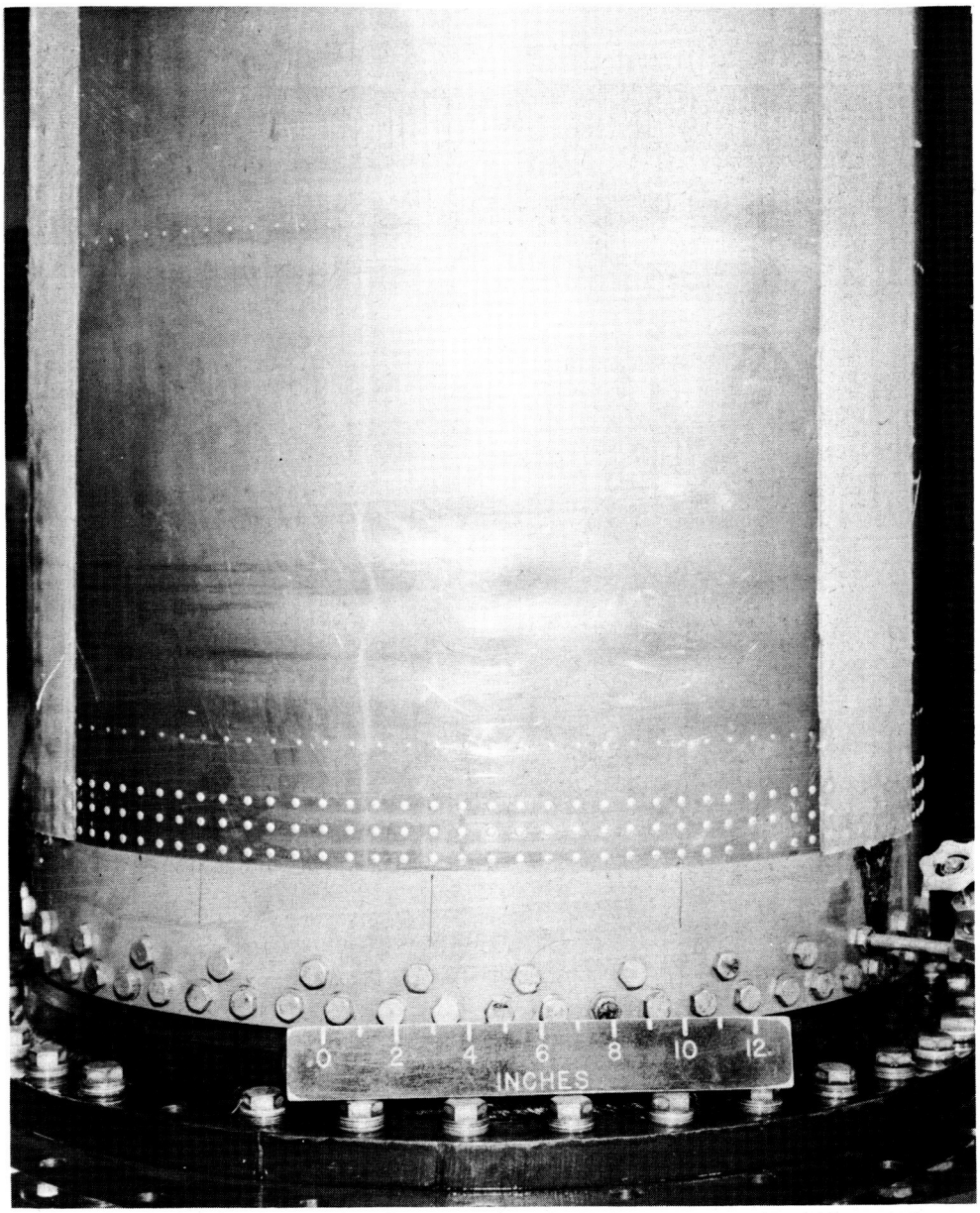

L-59-2983

(c) Local buckling at large value of internal pressure. Note moderate radii of curvature around perimeter of local buckles. $\frac{\sigma}{E}\frac{R}{t} = 0.552$; $\frac{p}{E}\left(\frac{R}{t}\right)^2 = 0.931$.

Figure 6.- Concluded.

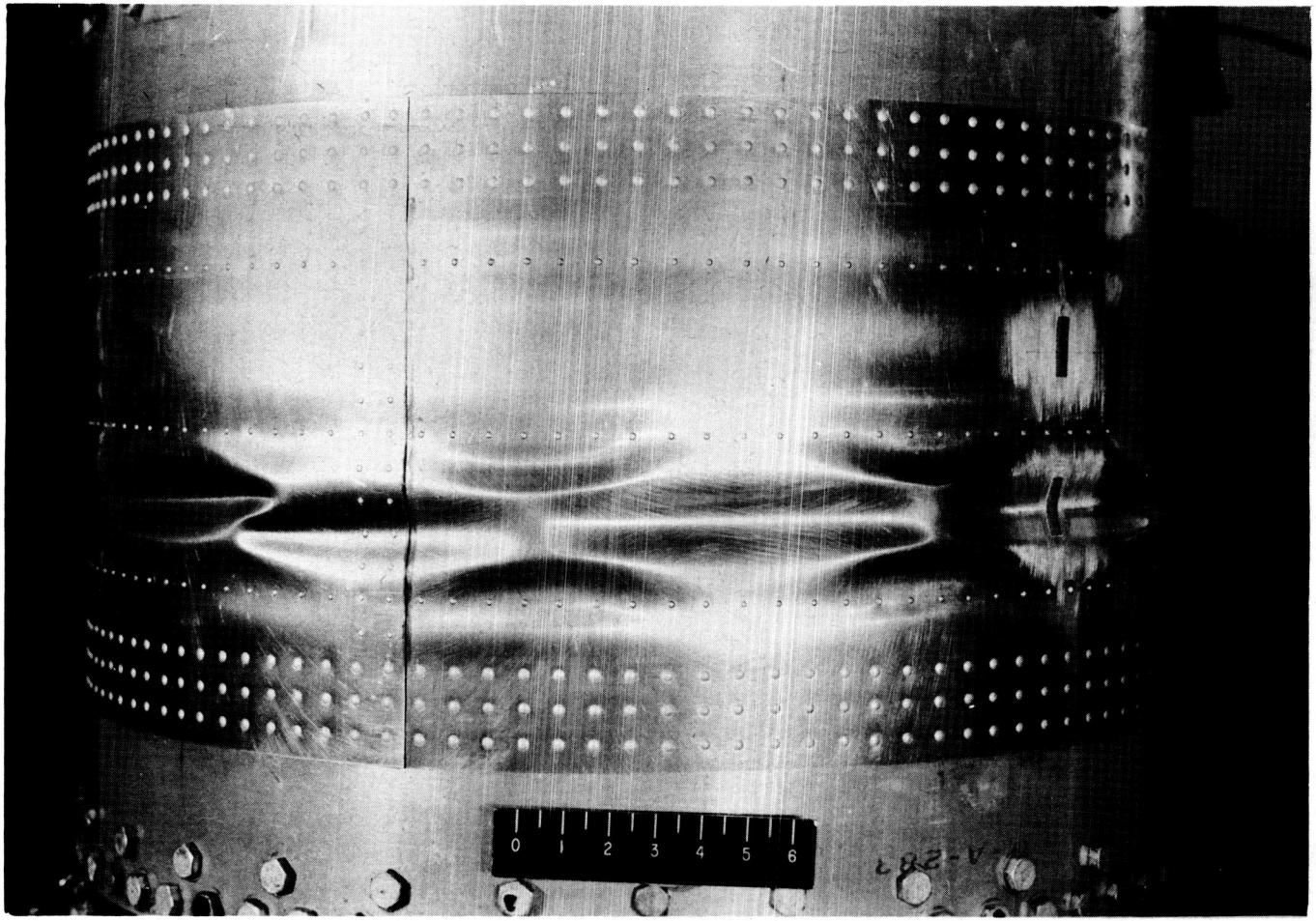

L-59-3723

Figure 7.- Appearance of local buckles after loading beyond the buckling stress. $\frac{R}{t} = 782$; $\frac{l}{R} = 0.246$; $\frac{p}{E}\left(\frac{R}{t}\right)^2 = 1.141$.